Rapid Field-Cycling MRI using Fast Spin-Echo

Rapid Field-Cycling MRI using Fast Spin-Echo

P. James Ross, Lionel M. Broche, David J. Lurie

Aberdeen Biomedical Imaging Centre, Musculoskeletal group, School of Medicine and Dentistry, University of Aberdeen, UK

Corresponding author: james.ross@abdn.ac.uk

Tel: +44 (0)1224-553206

Mail: James Ross, Biomedical Imaging Centre, Foresterhill, University of Aberdeen, Scotland, UK, AB25 2ZD

Keywords: field-cycling, relaxometric imaging, dispersion curve, quadrupole peaks.

Word Count:

Abstract: 196

Document: 2422

Abstract

Purpose: Fast Field-Cycling MRI (FFC-MRI) is a technique which promises to expand upon the diagnostic capabilities of conventional MRI by allowing the main field, B_0, to be varied during a pulse sequence, allowing access to new types of endogenous contrast. This necessitates longer scan times however, which can limit the technique's application to clinical research. In this paper an adaptation of the Fast Spin Echo pulse sequence for use with FFC-MRI is presented, known as Field-Cycling Fast Spin-Echo (FC-FSE). This technique allows much faster image acquisition, thus shortening scan times significantly.

Methods: Image quality and relaxometric accuracy were assessed by comparison of phantom images with data obtained using conventional techniques. As proof of principle, relaxometric images were obtained from the thighs of a human volunteer.

Results: Image quality remains good for speed-up factors of up to 4-fold. The accuracy of relaxometry data is in good agreement with conventional techniques. Results from a volunteer study were encouraging, demonstrating that the technique is sensitive enough to detect quadrupole peaks in-vivo.

Conclusions: The technique has been demonstrated in phantom experiments with little loss of image quality or relaxometric accuracy. Initial in-vivo results pave the way for future clinical studies.

Introduction

Fast Field-Cycling NMR (1) (FFC-NMR) is a well established technique that allows probing the variation of NMR relaxation rates with the Larmor frequency (or equivalently magnetic field strength). The relaxation parameter most commonly investigated is the longitudinal relaxation rate R_1, which typically has a strong dependence on field strength. Plots of R_1 against Larmor frequency are known as dispersion plots, and have a wide range of applications ranging from solid-state physics to the biological sciences. One such application of FFC-NMR is in the study of proteins in which ^{1}H-^{14}N cross relaxation effects may manifest as significant increases in R_1 occurring at specific NMR frequencies, generating peaks in the dispersion plot (2). In such samples these 'quadrupole peaks' can provide useful information on protein dynamics and concentration (3,4) which can be advantageously exploited in medical contexts. For instance FFC-NMR has shown recent promise in the characterisation of osteoarthritis (5). While FFC-NMR remains a useful tool for investigating R_1, the maximum sample size that commercially-available FFC NMR relaxometers can support is typically a few millilitres. This technique requires the collection of biopsies which limits the application of FFC-NMR for use in-vivo.

Fast Field-Cycling MRI (FFC-MRI) is a recently developed technique that aims to perform FFC-NMR on an MRI scanner, enabling the study of patients without intervention (6). Our team has built three such FFC-MRI scanners, two of which are whole-body sized. One limitation of FFC-MRI is the long scan time required by the acquisition of data over different values of B_0, particularly if R_1 measurement is to be performed. Previous work has demonstrated relaxometric imaging where FFC-MRI is used to manipulate image contrast, for example to obtain "protein contrast" images by careful choice of the evolution field (7). In the work of Ungersma et al. (8) , cross relaxation effects were observed using FFC-MRI in protein gel phantoms and T_1

dispersion contrast demonstrated in-vivo. Another approach is to use PRESS localisation (9) to obtain signal from a specific volume and to deduce R_1. This method is much faster than relaxometric imaging but is limited to voxel based experiments rather than entire images. It also requires good tissue homogeneity over the region of interest.

A related technique, known as Delta Relaxation Enhanced MR (dreMR) (10) has been demonstrated at high field MRI, where a resistive magnet is used to offset the main magnetic field in order to derive new contrast from changes in R_1. In contrast to FFC-MRI, which relies upon the inherently large variation in R_1 present at low field, dreMR exploits the relative invariance of R_1 with B_0 in tissues at high field to enhance the contrast generated by exogenous contrast agents.

In this work we present an adaptation of the well-known Fast Spin-Echo (FSE) imaging sequence, alternatively known as RARE (11), for use with FFC-MRI, known as Field-Cycling Fast Spin-Echo (FC-FSE), with the aim of achieving relaxometric imaging in a whole body scanner in a fraction of the time than is currently possible using existing field-cycling imaging techniques. FSE-type sequences have previously been demonstrated in similar fields such as prepolarized MRI (12,13), and dreMR (14), demonstrating its viability for field-cycling techniques.

In this report we have evaluated our sequence against conventional spin-echo imaging and validated R_1 dispersion plots obtained from phantoms against results obtained using a commercial fast field-cycling relaxometer. We have also demonstrated an initial proof of concept in a human volunteer.

Methods

A full description of FFC-NMR and its applications can be found in references (1,15) and a review of its extension to MRI is described in reference (6). The general basis for both FFC-NMR and FFC-MRI is that the primary magnetic field B_0, which is typically held static in conventional magnetic resonance, is now deliberately switched to different levels during the pulse sequence. A general field-cycling pulse sequence

can be described in terms of three periods: polarisation, evolution and detection. During polarisation the field is typically held at its maximum value B_0^P in order to increase the longitudinal magnetisation M_z. Immediately following polarisation the magnetic field is ramped to a chosen evolution field B_0^E where the spins undergo relaxation with a time constant R_1^E. Finally the field is returned to the scanner's native field B_0^D where the NMR signal is detected. As detection occurs at the same field regardless of B_0^E the system need not be adjusted or retuned for each new field. For cases where the switching time between magnetic fields occurs on a timescale much shorter than the T_1 of the sample the technique is then known as Fast Field Cycling (FFC). FFC is typically accomplished using either an electromagnet to rapidly vary the field experienced by the sample or by physically shuttling the sample within in the fringe field of a permanent magnet to accomplish the same result. FFC-MRI systems are generally of the former design given the practical difficulty of shuttling large, or living samples in short time periods.

Materials

All imaging was carried out using a home-built, field-cycling, whole-body imager (16). The imager is comprised of a permanent magnet (Field Effects Inc., MA, USA) which provides a detection field of 59 mT and a coaxial saddle-shaped resistive coil (Magnex Scientific Ltd., UK) that enables field-cycling through field compensation. The effective B_0 range of this system is 1 mT to 120 mT.

The system is controlled using a commercial console (SMIS Ltd., UK) and is equipped with a 1-kW peak power RF amplifier (Marconi Ltd, UK). Images were obtained using a 30-cm inner diameter transmit/receive Helmholtz RF head coil. To validate the accuracy of R_1 measurements FFC-MRI results were compared against those obtained from a FFC-NMR commercial bench-top relaxometer (SMARtracer, Stelar s.r.l, Italy).

Sequence Design

The FC-FSE pulse sequence was developed by combining a conventional inversion-recovery fast spin-echo sequence with a field-cycling step which takes place during the recovery period (Figure 1). Selective 5-lobe sinc RF pulses were used for

excitation and selective Gaussian RF pulses were used for refocusing, both using a bandwidth of 1.5 kHz. Crusher gradients were applied on either side of the refocusing pulses to avoid spurious out-of-slice signal. Inversion was performed using a selective hyperbolic secant pulse with duration of 10 ms which, along with the selective excitation and refocusing pulses, enabled interleaved multislice acquisitions. Phase encoding was arranged in a centric ordered fashion in order to retain maximum SNR and T_1 contrast, at a cost of spatial resolution at higher echo-train lengths (ETL). Hardware constraints limited the minimum echo spacing to approximately 34 ms. For this reason implementations of the sequence with an ETL greater than 8 were impractical due to SNR constraints. During image reconstruction a first-order phase correction was applied in order to correct for imperfect rewinder gradient pulses.

Image Quality Evaluation

Image quality was tested using a 200-mm diameter circular resolution phantom filled with a solution of 0.2-mM $MnCl_2$ prepared in deionised water (Figure 2). The image quality obtained using the FC-FSE sequence was qualitatively evaluated by collecting three images using echo train lengths of 2, 4 and 8 and comparing them against a conventionally acquired spin-echo image using a field of view of 240 x 240 mm, matrix size 128 x 128, slice thickness 20 mm, TE 36 ms, TR 1000 ms, evolution field 30 mT, evolution time 150 ms, echo spacing 36 ms and NEX 4.

Relaxometry Measurement Validation

Two phantoms were prepared for validating R_1 measurements. The first phantom consisted of 100 mL 15 % w/v Bovine Serum Albumin (BSA) cross-linked with 15% glutaraldehyde and 0.05-mM $MnCl_2$ prepared in deionised water. The second phantom consisted of 100 mL 0.2-mM $MnCl_2$ prepared in deionised water. All reagents were sourced from Sigma Aldrich, UK. The phantom compositions were chosen to have similar R_1 dispersion values as would be expected from human muscle tissue with and without quadrupole signal. Relaxometric phantom images were obtained with parameters as follows: field of view of 155 x 155 mm, matrix size 64 x 64, slice thickness 30 mm, TE 34 ms, TR 1000 ms, echo spacing 34 ms, ETL 4, evolution time 180 ms and NEX 4. 34 evolution field strengths were used, ranging from 34 to 72 mT and including the reference field at 59 mT. A delay of 60 ms was

included immediately following field-cycling and prior to excitation to allow for field stabilisation. The total scan time was 37 minutes.

The duration of the post field-cycling delay was chosen to ensure that no artefacts due to B_0 instability manifested in images. Such artefacts range from blurring in moderate cases, resulting from B_0 'ringing' occurring in the readout period, to a near total loss of signal in severe cases due to irreversible spin dephasing following excitation. Figure 3 shows the effects of shorter delays. With a delay of 60 ms no degradation is evident. When the delay is shortened to 40 ms there is a visible loss of signal and slight blurring. In the extreme case of a 15 ms delay there is a near complete loss of signal.

Initial In-Vivo Evaluation

FC-FSE images were obtained of the thigh of an adult male human volunteer. The acquisition parameters used were: field of view 320 x 320 mm, matrix size 128 x 128, slice thickness 20 mm, TE 36 ms, TR 1000 ms, echo spacing 36 ms, ETL 4, NEX 3, evolution time 150 ms. 25 evolution field strengths were used, ranging from 40 mT to 70 mT, including a reference field image acquired at 59 mT, which is shown in Figure 5 (left). The post field-cycling delay was 60 ms. Total scan time was 40 minutes.

All raw data was exported, reconstructed and analysed using in-house software written using MATLAB R2012a (The MathWorks, Inc., MA, USA).

Results

Experiments were carried out to confirm the accuracy and robustness of R_1 measurements, to ensure that images obtained using the sequence were artefact free and to test the feasibility for use on human subjects.

Image Quality

Image quality was assessed by visually comparing images obtained using FC-FSE with a range of echo train lengths, with a constant evolution field of 30 mT, against a conventionally acquired spin-echo image (Figure 2). For low-speed up factors using only two echoes there was little observable difference between the FC-FSE image and the spin-echo image. When using an ETL of 4 modest blurring was present while for ETLs of 8 and above severe blurring was evident. For the spin echo image

A the SNR was determined to be 17.4. The SNRs for the three FC-FSE images B-D was 17.7, 16.8 and 13.8 respectively. All images obtained exhibited significant intensity inhomogeneity which has been attributed to B_1 inhomogeneity. This was not deemed likely to have a significant impact on R_1 measurement accuracy as the distortion was consistent throughout all experiments and an adiabatic pulse was used for inversion.

Relaxometry

Images were acquired of a setup consisting of two phantoms, one containing a solution of $MnCl_2$ and the second containing a solution of crosslinked BSA, across a range of field strengths. Each image corresponded to a specific field strength. From these images R_1 dispersion plots were derived by manually selecting a region of interest and then using the mean voxel value within that area to determine R_1 at the evolution field corresponding to that image, using a two-point method (17,18). For each solution two dispersion curves were calculated and compared: the first was acquired using the method described and the second was taken from the commercial relaxometer (Figure 4). The results obtained using the FC-FSE sequence and those obtained using the relaxometer showed good agreement for both the test objects.

In-Vivo

As a proof-of-principle, images were acquired of a human volunteer's thigh using the FC-FSE sequence. Regions of interest were drawn around a region containing muscle tissue (Figure 5) and a muscle-free region containing fat. Dispersion curves were derived using the same method as for the relaxometry phantoms. The dispersion curve for the region of muscle showed distinct quadrupole peaks centred around 2.1 MHz and 2.7 MHz. These can be attributed to the presence of immobile protein within the muscle. The dispersion curve for the region containing no muscle showed no quadrupole peaks (data not shown) as this tissue contains much less immobile protein.

Discussion and Conclusion

We have presented a successful implementation of a field-cycling fast spin-echo imaging sequence and have demonstrated that it can be used to derive R_1 dispersion curves with comparable accuracy to conventional FFC-NMR methods. Speed-up factors of up to four-fold have been demonstrated with little or no image distortion and little change in SNR. Careful choice of phase encoding order enables the trade-off of speed-up factor against image resolution.

The technique has been demonstrated to be sufficiently sensitive to detect quadrupole peaks in phantoms and in-vivo and their location is in agreement with results in the literature (2). Furthermore the relatively short scan times permit human studies to be performed in a reasonable timeframe. For comparison the in-vivo results described in this work, which took approximately 40 minutes to acquire, would have taken nearly 2 hours 40 minutes to obtain using previous methods, making human studies infeasible.

There are a number of potential avenues where future work might build upon the results described here. The ability to directly measure protein concentration through detection of quadrupole peaks has potential application in the study of sarcopenia and other muscle wasting conditions. Alternatively, it has been shown in an in vitro model of thrombosis (3) that protein concentration can be used as a direct measure of fibrin concentration. This highlights a potential application of FFC-MRI in the detection and assessment of thrombosis. Even in the absence of quadrupole peaks, the ability to unlock R_1 dispersion may offer benefits over conventional methods. It has long been known that the R_1 dispersion of human tissue changes with disease. Koenig et al. first described significant differences in cancerous human breast compared to healthy tissue (19). In this context FFC-MRI might provide a means of characterisation and grading of tumours.

In conclusion this report describes a rapid and robust method for relaxometric imaging on a FFC-MRI scanner. It is a combination of the well-known RARE imaging sequence with the fast field-cycling technique and provides a means of measuring R_1 dispersion data across the full evolution field range permitted by the scanner with a minimum of image artefacts and with a speed up factor of up to 4 fold compared to spin-echo or gradient echo techniques. This paves the way for a range of FFC-MRI applications in clinical research where scan time can be a critical factor.

References

1. Kimmich R. Field-cycling NMR relaxometry. Prog. Nucl. Magn. Reson. Spectrosc. 2004:257–320. doi: 10.1007/978-3-642-60582-6.

2. Winter F, Kimmich R. Spin lattice relaxation of dipole nuclei (I = 1/2) coupled to quadrupole nuclei (S = 1). Mol. Phys. 1982;45:33–49. doi: 10.1080/00268978200100031.

3. Broche LM, Ismail SR, Booth NA, Lurie DJ. Measurement of fibrin concentration by fast field-cycling NMR. Magn. Reson. Med. 2012;67:1453–7. doi: 10.1002/mrm.23117.

4. Jiao X, Bryant RG. Noninvasive measurement of protein concentration. Magn. Reson. Med. 1996;35:159–61.

5. Broche LM, Ashcroft GP, Lurie DJ. Detection of osteoarthritis in knee and hip joints by fast field-cycling NMR. Magn. Reson. Med. 2012;68:358–62. doi: 10.1002/mrm.23266.

6. Lurie DJ, Aime S, Baroni S, Booth NA, Broche LM, Choi C-H, Davies GR, Ismail S, Ó Hógáin D, Pine KJ. Fast field-cycling magnetic resonance imaging. Comptes Rendus Phys. 2010;11:136–148. doi: 10.1016/j.crhy.2010.06.012.

7. Carlson JW, Goldhaber DM, Brito A, Kaufman L. MR relaxometry imaging. Work in progress. Radiology 1992;184:635–9.

8. Ungersma SE, Matter NI, Hardy JW, Venook RD, Macovski A, Conolly SM, Scott GC. Magnetic resonance imaging with T1 dispersion contrast. Magn. Reson. Med. 2006;55:1362–71. doi: 10.1002/mrm.20910.

9. Pine KJ, Davies GR, Lurie DJ. Field-cycling NMR relaxometry with spatial selection. Magn. Reson. Med. 2010;63:1698–702. doi: 10.1002/mrm.22346.

10. Alford JK, Rutt BK, Scholl TJ, Handler WB, Chronik BA. Delta relaxation enhanced MR: improving activation-specificity of molecular probes through R1 dispersion imaging. Magn. Reson. Med. 2009;61:796–802. doi: 10.1002/mrm.21933.

11. Hennig J, Nauerth A, Friedburg H. RARE imaging: a fast imaging method for clinical MR. Magn. Reson. Med. 1986;3:823–33.

12. Kegler C, Seton HC, Hutchison JMS. Prepolarized fast spin-echo pulse sequence for low-field MRI. Magn. Reson. Med. 2007;57:1180–4. doi: 10.1002/mrm.21238.

13. Matter NI, Scott GC, Venook RD, Ungersma SE, Grafendorfer T, Macovski A, Conolly SM. Three-dimensional prepolarized magnetic resonance imaging using rapid acquisition with relaxation enhancement. Magn. Reson. Med. 2006;56:1085–95. doi: 10.1002/mrm.21065.

14. Hoelscher UC, Lother S, Fidler F, Blaimer M, Jakob P. Quantification and localization of contrast agents using delta relaxation enhanced magnetic resonance at 1.5 T. MAGMA 2012;25:223–31. doi: 10.1007/s10334-011-0291-6.

15. Anoardo E, Galli G, Ferrante G. Fast-field-cycling NMR: Applications and instrumentation. Appl. Magn. Reson. 2001;20:365–404. doi: 10.1007/BF03162287.

16. Lurie DJ, Foster MA, Yeung D, Hutchison JM. Design, construction and use of a large-sample field-cycled PEDRI imager. Phys. Med. Biol. 1998;43:1877–86.

17. Lin MS, Fletcher JW, Donati RM. Two-point T1 measurement: wide-coverage optimizations by stochastic simulations. Magn. Reson. Med. 1986;3:518–33.

18. Broche LM, Ross PJ, Pine KJ, Lurie DJ. Rapid multi-field T1 estimation algorithm for Fast Field-Cycling MRI. J. Magn. Reson. 2014;238:44–51.

19. Koenig SH, Brown RD. Determinants of Proton Relaxation Rates in Tissue. Magn. Reson. Med. 1984;1:437–449. doi: 10.1002/mrm.1910010404.

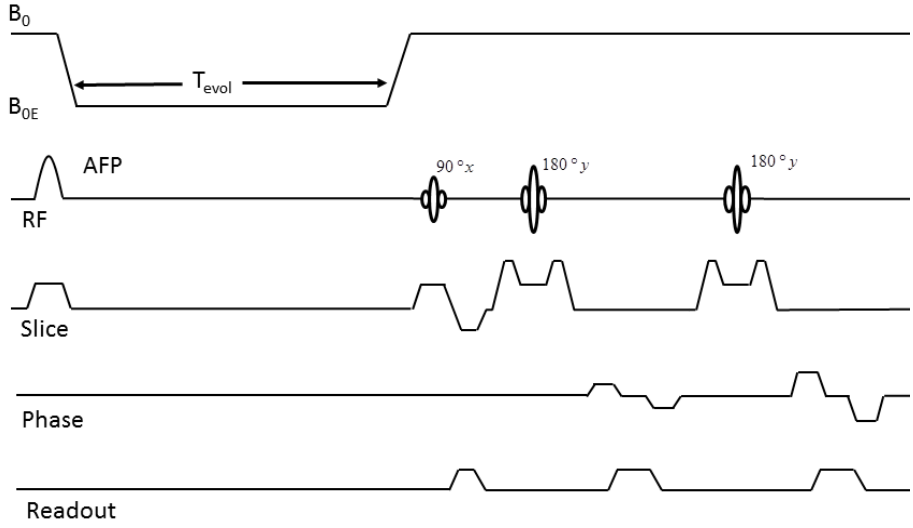

Figure 1: Timing of the FC-FSE sequence with an ETL of 2, showing inversion by means of an adiabatic full-passage (AFP) RF pulse, field-cycling preparation and finally excitation and readout.

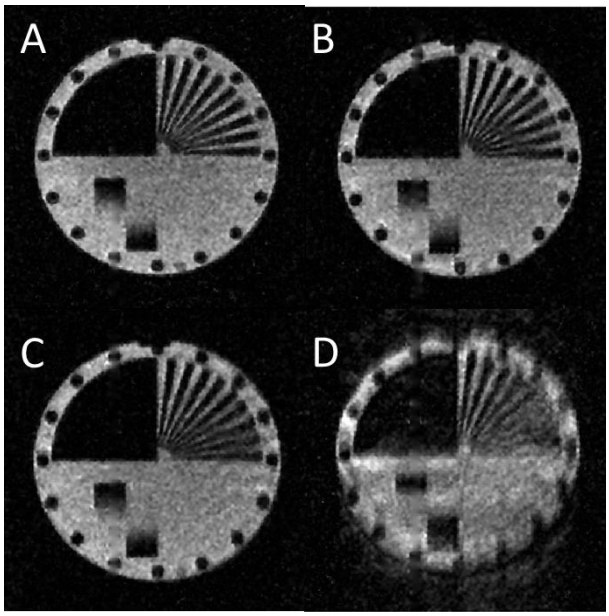

Figure 2: Resolution phantom images obtained at an evolution field of 30 mT. Image A was obtained using a conventional spin-echo sequence (i.e. ETL = 1) while images B-D were obtained using the FC-FSE sequence with ETLs of 2, 4 and 8 respectively Non-uniform image intensity (top to bottom) can be observed in all the images, which has been attributed to B_1 inhomogeneity, and is independent of the speed-up factor used.

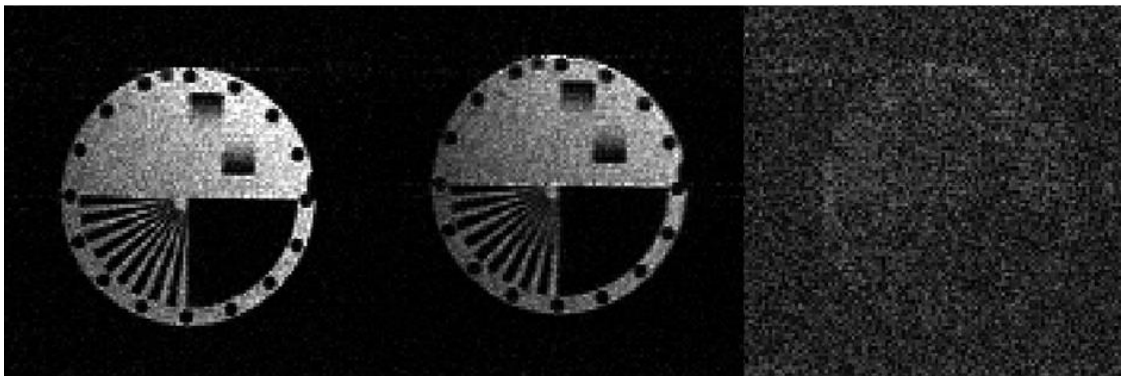

Figure 3: Images collected at an evolution field of 30 mT demonstrating the need for a delay immediately following field-cycling to allow the resistive magnet to settle. The settling times from left to right were 60 ms, 40 ms and 15 ms.

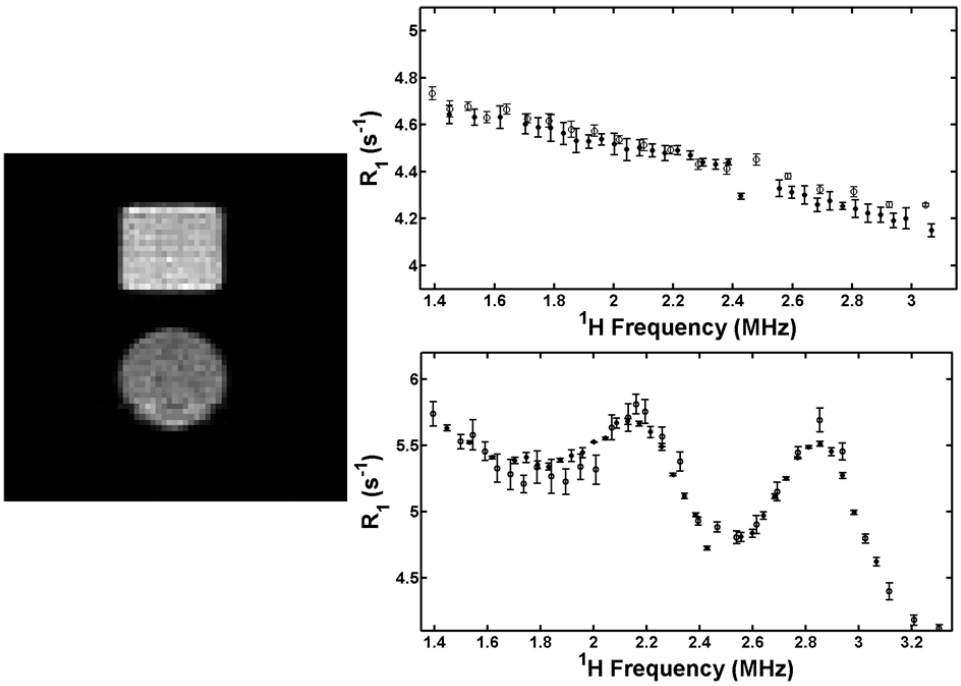

Figure 4: Left: phantom images used to validate the accuracy of R_1 measurements. The square phantom consists of a solution of 0.2-mM of $MnCl_2$ while the circular phantom consists of 15% v/w bovine serum albumin cross-linked with 15% glutaraldehyde. Right: Dispersion curves from the $MnCl_2$ solution (top) and BSA solution (bottom) derived using the FC-FSE sequence (triangles) compared against a dispersion plot from a commercial relaxometer (open circles).

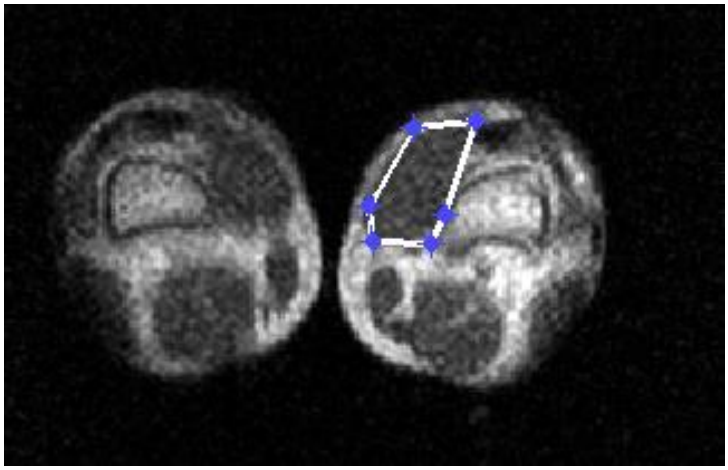

Figure 5: Image of a volunteer's thighs (left) acquired using an evolution field of 59 mT. This image is one of a set of images, each with a different evolution field, from which a dispersion curve was derived from the delineated region of interest (right). Note the clear quadrupole peaks (arrows), arising due to the immobile protein in the marked region of muscle.